Sussex Research Online

Responses of the terrestrial ecosystem productivity to droughts inside China

Article (Supplemental Material)

Li, Jianguo, Wang, Yi and Liu, Lili (2020) Responses of the terrestrial ecosystem productivity to droughts inside China. Frontiers in Earth Science, 8 (a59). pp. 1-13. ISSN 2296-6463

This version is available from Sussex Research Online: http://sro.sussex.ac.uk/id/eprint/90024/

This document is made available in accordance with publisher policies and may differ from the published version or from the version of record. If you wish to cite this item you are advised to consult the publisher's version. Please see the URL above for details on accessing the published version.

Copyright and reuse:
Sussex Research Online is a digital repository of the research output of the University.

Copyright and all moral rights to the version of the paper presented here belong to the individual author(s) and/or other copyright owners. To the extent reasonable and practicable, the material made available in SRO has been checked for eligibility before being made available.

Copies of full text items generally can be reproduced, displayed or performed and given to third parties in any format or medium for personal research or study, educational, or not-for-profit purposes without prior permission or charge, provided that the authors, title and full bibliographic details are credited, a hyperlink and/or URL is given for the original metadata page and the content is not changed in any way.

http://sro.sussex.ac.uk

Responses of the terrestrial ecosystem productivity to droughts inside China

Jianguo Li [1,2*], Yi Wang[2,3*], Lili Liu[1]

1. School of Geography, Geomatics, and Planning, Jiangsu Normal University, Xuzhou, Jiangsu 221116, China;

2. Department of Geography, School of Global Studies, University of Sussex, Falmer, Brighton, UK BN1 9QJ

3. Department of Earth System Science, Institute for Global Change Studies, Tsinghua University, Beijing 100084, China

Supplementary Materials

S1. Our CASA model

The NPP inside China during the period of 1982-2012 is estimated using the CASA model (Zhu et al., 2006). The calculation model is detailed by the following two equations:

$$NPP(x,t) = APAR(x,t) \times \varepsilon(x,t) \quad (1)$$

$$APAR(x,t) = SOL(x,t) \times FPAR(x,t) \times 0.5 \quad (2)$$

where *NPP(x,t)* is the NPP at pixel *x* (gC/m^2/yr) at month t; *APAR(x,t)* is the photosynthetically active radiation at month *t* and pixel *x* (gC/m^2/month), and *ε(x, t)* is the active light use efficiency at month *t* and pixel *x* (gC/MJ). SOL(x,t) is the total solar radiation at month t and pixel x (MJ/m^2/month). FPAR(x,t) is the fraction of photosynthetically active radiation at month t and pixel x, representing the percentage of photosynthetically active radiation absorbed by plant. Different from the ordinary CASA model (Fang et al., 2003), our FPAR has been estimated using the linear relationship between FPAR and normalized vegetation index based on previous studies

(Hunt Raymond, 1994; Zhu et al., 2007). A factor of 0.5 is used to reflect the proportion of active solar radiation to total solar radiation. Also, in contrast to the ordinary CASA model, the maximum efficiency of light energy utilization of each vegetation type in China is determined from a previous modeling study (Zhu et al., 2006). Their model provides a more reliable estimate of Chinese NPP, and has been widely applied by other studies (Mu et al., 2013; Zhang et al., 2009). Furthermore, our potential evapotranspiration (PET) is determined using the Penman-Monteith method, which is verified as the optimum method to estimate China's PET (Yang et al., 2016).

S2. The meteorological and land cover dataset

All meteorological data downloaded from the Data Center of Chinese Meteorological Administration is imported into ArcGIS 10.2 software to get the location of each meteorological station (see Fig. 1 in the article), and then interpolated to obtain maps of monthly precipitation, monthly mean temperature, and monthly total solar radiation using the inverse distance weight method (Bartier and Keller, 1996). Land-cover images are from the SPOT-VGT site (http://free.vgt.vito.be/) and the V005 MODIS Land Cover Dynamics (MCD12Q2) product (https://modis.gsfc.nasa.gov/) based on the land-cover classification system of International Geosphere-Biosphere Programme (IGBP). The coordinates, projection, and spatial resolution of land-cover and other interpolation maps are consistent with the NDVI dataset.

S3. Two droughts' indices

The drought indices (SPI and SPEI) are originated from observed dataset from meteorological stations inside China (see Fig.1 in the article). Two drought indices at each station are obtained by using "spei" tool from "SPEI" package in R software (Beguería et al., 2014; Vicente-Serrano et al., 2010), and then interpolated to produce SPI and SPEI maps using the inverse distance weight

method (Bartier and Keller, 1996). The map projection and grid cell size of SPI and SPEI maps are the same as the NPP map. According to the SPI calculation by Kumar et al. (2009), a negative SPI value represents less rainfall (dry conditions), whereas a positive SPI value means more rainfall (wet conditions). The smaller the SPI is, the severer the drought is. When the SPI is less than -2, a severe drought occurs. Compared with the SPI, the SPEI considers the status of land surface PET, and is a relatively comprehensive drought index (Vicente-Serrano et al., 2010). The SPI and SPEI indices are characterised by multi-timescales, such as 3-, 6-, 9-, and 12-month (and longer) timescales. The drought status over a 3-month period can be identified by using the SPI3 and SPEI3 images. The multi-timescale feature is useful in studying a response time or the lagging effect of an ecosystem to droughts (Beguería et al., 2014; Zarei and Eslamian, 2017). All our spatial analyses and statistics are performed by using R, ArcGIS 10.2 (ESRI, USA), and ENVI 5.3 (ESRI, USA) software.

S4. Our statistical methods

S4.1 The drought frequency

The drought frequency is defined as the ratio of the months of drought to the total months of observation period and is calculated as:

$$P = \frac{D_{(t)}}{T} \times 100\% \quad (3)$$

where P is drought frequency (%), $D_{(t)}$ is the total months at drought level t, and T is the total months of observation. In this study, T equals to 372 months.

S4.2 The correlation analysis

The correlation between the NPP and drought indices have been examined using Pearson's method. The equation is:

$$r = \frac{\sum (x_i - \bar{x})(y_i - \bar{y})}{\sqrt{\sum (x_i - \bar{x})^2 \sum (y_i - \bar{y})^2}} \quad (4)$$

where x_i is the monthly drought index (SPI/SPEI) and y_i is the monthly NPP.

S4.3 The regression/trend analyses

K-slope is used to reflect the relative variation of monthly NPP per drought index changes, and is calculated as:

$$K_{Slope} = \frac{n \times \sum (x_i \times y_i) - \sum x_i \sum y_i}{n \times \sum x_i^2 - (\sum x_i)^2} \quad (5)$$

where k_{Slope} is the slope of the unary linear regression model; x_i is the monthly NPP and y_i is the monthly drought index; n is 372 (see Fig. 7 in the article). In order to determine the annual NPP trend (see Fig. 9 in the article), the same equation (5) is used. However, in the trend analysis, x_i is the annual NPP from 1982 to 2012, and y_i is time in year; n is 31.

S4.3 The contributions of the SPI/SPEI to China's NPPs across different timescales

A unary linear regression model is constructed to determine the quantitative relationship between SPI/SPEI and China's NPP across three timescales (3-month,6-month and 12-month). The equation takes the form below:

$$y = ax + b \quad (6)$$

where, y is NPP; x is the driving force, here is drought index (SPI/SPEI).

S4.4 The contribution of droughts to China's monthly NPP variation

The coefficient of determination of the unary linear regression model (r-square) indicates the proportion of the variance of the dependent variable explaining the variance of independent variable, and can be used to represent the contribution level of drought on the NPP variation. The

formula is:

$$R^2 = (1 - \frac{SS_{res}}{SS_{tot}}) \times 100\% \quad (7)$$

where R^2 is the contribution level (%), SS_{res} is the sum of the squares of error of the unary linear regression model, and SS_{tot} is the sum squares. Formulas (3), (4), (5), and (6) were run on R version 3.4.2 software.

S5. The validation of our analyses

The drought indices are diverse (Hou et al., 2007; Yang et al., 2017). Compared with the Palmer Drought Severity Index (PDSI), the flexible timescales of the SPI and SPEI indices are beneficial in assessing the relationships between drought and monthly NPP variability over multiple timescales. The ecological responses of drought index are different among multiple timescales. The SPEI1 and SPI1 indices are used to reflect the water distribution in land surface with less significant impact on vegetation activity. However, at 6-month and longer timescales of the SPEI and SPI indices can reflect the drying-wetting alteration and long-term water distribution, resulting in a remarkable influence on vegetation activity (Mathbout et al., 2018). The correlation between the SPI and SPEI is examined at 3-, 6- and 12-month timescales (see Fig. S1 in supplementary material). The mean correlation coefficient is 0.57 at the 3-month timescale and decreases to 0.55 at the 12-month timescale. Stronger relationships between the two drought indices have been found in eastern China, suggesting that our results in those areas are more reliable (see Fig. S1 in supplementary material). In addition, the SPEI is more sensitive than the SPI in explaining the responses of the monthly NPP variation to drought in China due to larger extent and stronger correlation of significant relationships between them (see Figs. 6 and 7 in the article).

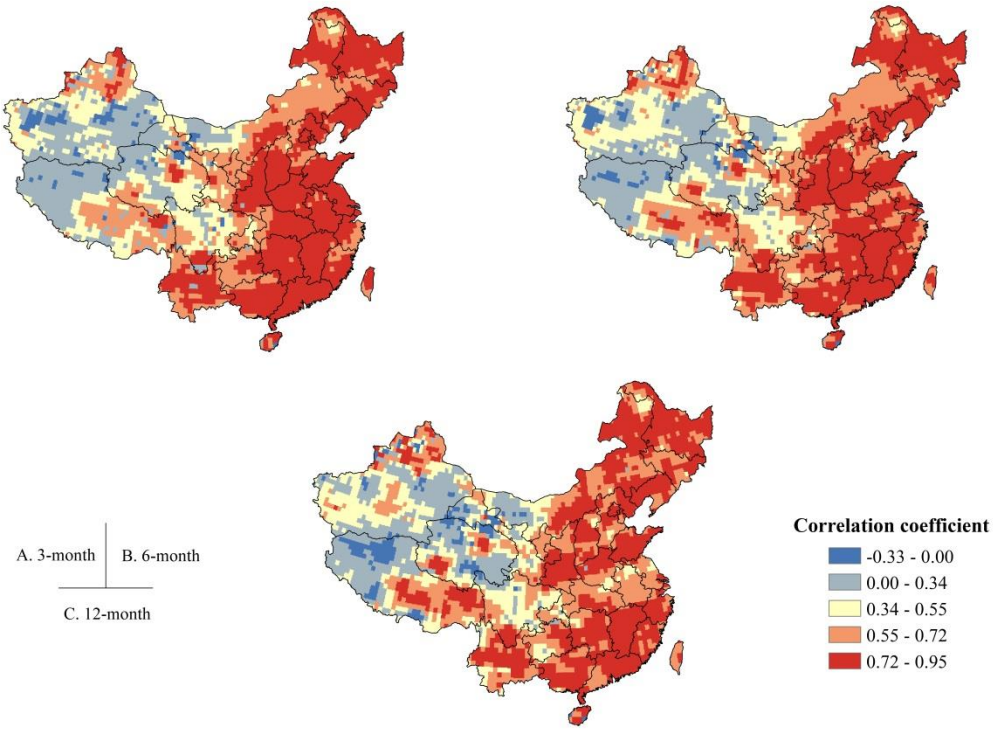

Fig. S1 Correlation coefficients between SPI and SPEI at (A) 3-month, (B) 6-month and (C) 12-month timescales

The mean monthly SPEI3 in China were extracted during the study period (see Fig. S2), revealing that drought usually occurs in summer. However, the humid periods during a given year tends to shorten and the drought periods tends to increase, indicating that China's climate generally tends to be dry, which is supported by Qian et al. (2014). Aridification during the summer has tended to aggravate sharply, especially in the past 15 years. In the summer of 1999, the SPEI3 decreased to -1, suggesting that moderate drought appeared across China (see supplementary material, Fig. S2). On the basis of Fig. S2A, the drought in northern China has tended to increase during the study period, which will cause a huge risk to the future localized NPP in China. Although, according to Fig. 3B and Fig. 8 in the article, interannual NPP inside China has tended to increase, a negative effect of water on the monthly NPP variation in southern China at the 3-month timescale has been found (see Fig. 7 in the article). This negative effect of

them is probably caused by frequent heavy rainfall in the summer of southern China at the shorter timescale, which however contributes little to interannual variability of the NPP in China. The increasing annual NPP trend inside China has been testified by many studies (Pei et al., 2013; Piao et al., 2005; Yuan et al., 2014). The main reasons are: 1) The advances in agricultural facilities, breeding, fertilization, and management all support the ecosystem production of farmland; 2) The NPP of natural ecosystems (forest, grass, and high mountains) continue to increase due to global warming and nitrogen deposition, which can compensate for the NPP losses caused by flooding (Zhan et al., 2015; Zhu et al., 2015); 3) The aridification does not reach a threshold that restricts vegetation activity in southern China, where radiation has been demonstrated as the main driving factor of vegetation activity (Nemani et al., 2003).

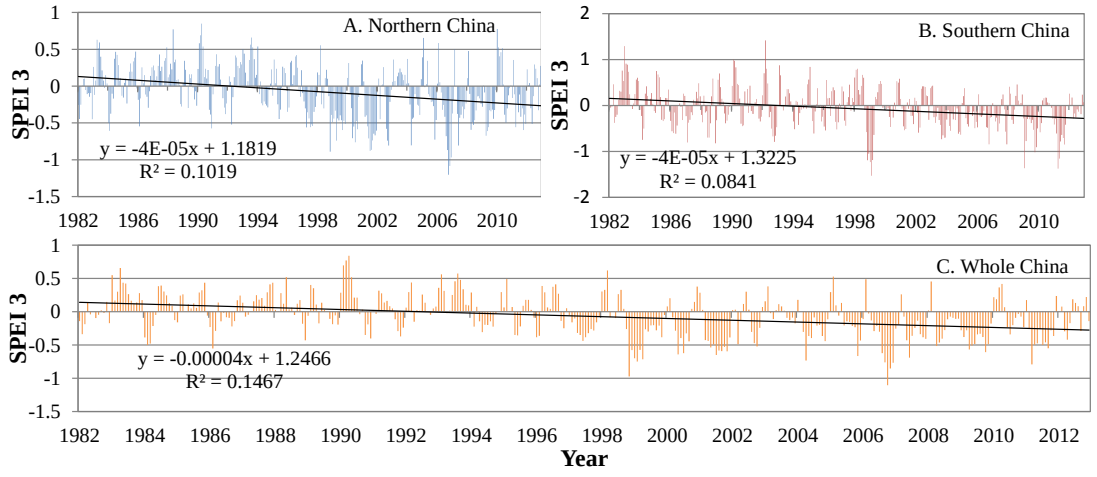

Fig. S2 Variations of SPEI3 index in China from 1982 to 2012. (A) For Northern China, (B) For Southern China, and (C) For the whole China. The regression lines are shown together with the actual SPEI3 time series in each panel.

S6. Chinese forestry data (1950-2013)

To find out what contribute to this long-term and substantial increase of annual total NPP inside China, we have downloaded the forest inventory data from Chinese Forestry Administration

Government website (http://www.forestry.gov.cn/portal/xdly/s/5197/content-931245.html) to investigate the changes of Chinese forest coverage (Fig. s3B) and farmland coverage (Fig. s3A), based on data from a previous study (Liu et al., 2014), and our derived NPP for corresponding plant functional types (Fig. s3C). Our results have showed that farmland cover has increased 5% (Fig. s3A), and forest cover has almost doubled from 1982 to 2012 (Fig. s3B), and the corresponding forest NPP has increased from 1452.3 TgC to 1565.19 TgC during this period (Fig. s3C). In addition, the farmland NPP has also increased for 896.51 TgC to 1066.53 TgC during the same period (Fig. s3C). We believe the long-term and substantial increase of total NPP inside China is linked to the government sponsored reforestation and the ever expanding agriculture activities over the last decades (Wang et al., 2017).

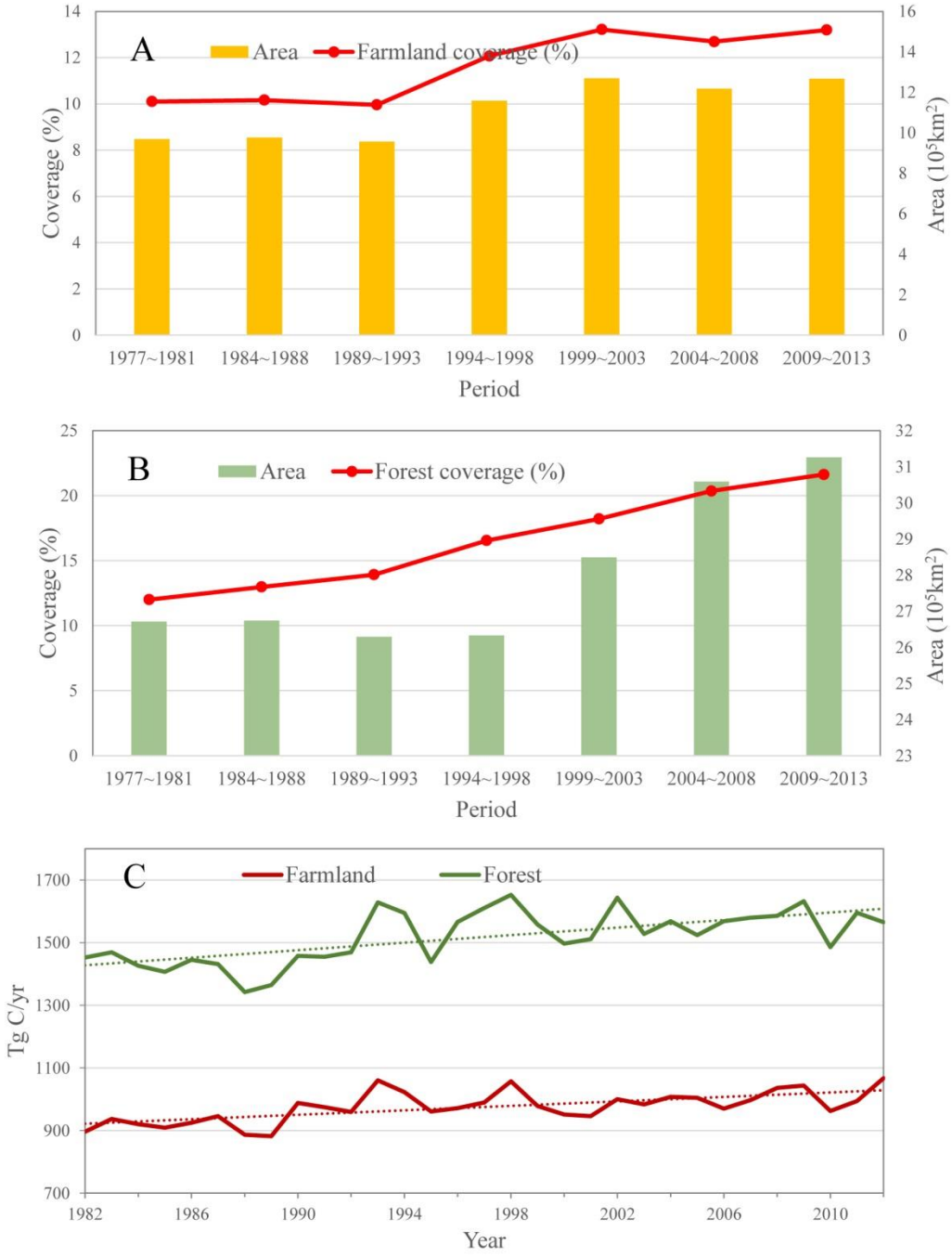

Insert Fig.s3 The timeseries of (A) Chinese farmland (Liu et al., 2014), (B) Chinese forestry (see supplementary material Table S1), and (C) Our derived NPP for corresponding plant functional types.

Table S1: Chinese forestry data for the period between 1950 and 2013 (Data source: 2010-2015 Chinese forestry development report, accessed online at

159 **http://www.forestry.gov.cn/portal/xdly/s/5197/content-931245.html)**

Periods between 1950 to 2013	Forest Area (km^2)	Forest Coverage (%)
1950～1962	2120000	8.90
1973～1976	2576000	12.70
1977～1981	2671000	12.00
1984～1988	2674000	12.98
1989～1993	2629000	13.92
1994～1998	2633000	16.55
1999～2003	2849000	18.21
2004～2008	3059000	20.36
2009～2013	3126000	21.63

160

161

162 **Reference:**

163 Bartier, P.M., Keller, C.P. (1996). Multivariate interpolation to incorporate thematic surface data using
164 inverse distance weighting (IDW). Computers & Geosciences, 22, 795-799.
165 http://dx.doi.org/10.1016/0098-3004(96)00021-0

166 Beguería, S., Vicente-Serrano, S.M., Reig, F., Latorre, B. (2014). Standardized precipitation
167 evapotranspiration index (SPEI) revisited: parameter fitting, evapotranspiration models, tools,
168 datasets and drought monitoring. International Journal of Climatology 34, 3001-3023.
169 http://dx.doi.org/10.1002/joc.3887

170 Fang, J., Piao, S., Field, C.B., Pan, Y., Guo, Q., Zhou, L., Peng, C., Tao, S. (2003). Increasing net
171 primary production in China from 1982 to 1999. Frontiers in Ecology and the Environment., 1,
172 293-297. https://www.jstor.org/stable/3868089

173 Hou, Y., He, Y., Liu, Q., Tian, G. (2007). The research on the drought indice. Chinese Journal of
174 Ecology, 26, 892-897 (in chinese).

175 Kumar, M.N., Murthy, C.S., Sai, M.V.R.S., Roy, P.S. (2009). On the use of Standardized Precipitation

Index (SPI) for drought intensity assessment. Meteorological Applications, 16, 381-389. http://dx.doi.org/10.1002/met.136

Liu, J., Kuang, W., Zhang, Z., Xu, X., Qin, Y., Ning, J., Zhou, W., Zhang, S., Li, R., Yan, C. (2014). Spatiotemporal characteristics, patterns, and causes of land-use changes in China since the late 1980s. Journal of Geographical Sciences 24, 195-210. https://xs.scihub.ltd/https://doi.org/10.1007/s11442-014-1082-6

Mathbout, S., Lopez-Bustins, J.A., Martin-Vide, J., Bech, J., Rodrigo, F.S. (2018). Spatial and temporal analysis of drought variability at several time scales in Syria during 1961–2012. Atmospheric Research, 200, 153-168. https://doi.org/10.1016/j.atmosres.2017.09.016

Mu, S., Zhou, S., Chen, Y., Li, J., Ju, W., Odeh, I. (2013). Assessing the impact of restoration-induced land conversion and management alternatives on net primary productivity in Inner Mongolian grassland, China. Global Planet Change, 108, 29-41. https://doi.org/10.1016/j.gloplacha.2013.06.007

Nemani, R., R. (2013). Climate-Driven Increases in Global Terrestrial Net Primary Production from 1982 to 1999. Science, 300, 1560-1563. https://doi.org/10.1126/science.1082750

Pei, F., Li, X., Liu, X., Lao, C. (2013). Assessing the impacts of droughts on net primary productivity in China. Journal of Environmental Management 114, 362-371. https://doi.org/10.1016/j.jenvman.2012.10.031

Piao, S., Fang, J., Zhou, L., Zhu, B., Tan, K., Tao, S. (2005). Changes in vegetation net primary productivity from 1982 to 1999 in China. Global Biogeochemical Cycles 19, 1605-1622. https://doi.org/10.1029/2004GB002274

Qian, C., Yu, J.Y., Chen, G. (2014). Decadal summer drought frequency in China: the increasing

influence of the Atlantic Multi-decadal Oscillation. Environmental Research Letters, 9, 124004. https://doi.org/10.1088/1748-9326/9/12/124004

Hunt, Raymond, E. (1994). Relationship between woody biomass and PAR conversion efficiency for estimating net primary production from NDVI. International Journal of Remote Sensing, 15, 1725-1729. https://doi.org/10.1080/01431169408954203

Vicente-Serrano, S.M., Beguería, S., López-Moreno, J.I. (2010). A Multiscalar Drought Index Sensitive to Global Warming: The Standardized Precipitation Evapotranspiration Index. Journal of Climate, 23, 1696-1718. https://doi.org/10.1175/2009JCLI2909.1

Wang, W., Ouyang, W., Hao, F., Liu, G. (2017). Temporal-spatial variation analysis of agricultural biomass and its policy implication as an alternative energy in northeastern China. Energy Policy, 109, 337-349. https://doi.org/10.1016/j.enpol.2017.06.068

Yang, Q., Li, M., Zheng, Z., Ma, Z. (2017). Regional applicability of seven meteorological drought indices in China. Science China: Earth Sciences, 60, 745-760. https://doi.org/10.1007/s11430-016-5133-

Yang, Y., Y. Cui, Y., Luo, X., Lyu, S., Traore, S. Khan, Wang. W. (2016). Short-term forecasting of daily reference evapotranspiration using the Penman-Monteith model and public weather forecasts, Agricultural Water Management, 177, 329-339. https://doi.org/10.1016/j.agwat.2016.08.020

Yuan, Q., Wu, S., Zhao, D., Dai, E., Chen, L., Zhang, L. (2014). Modeling net primary productivity of the terrestrial ecosystem in China from 1961 to 2005. Journal of Geographical Sciences 24, 3-17. https://doi.org/10.1007/s11442-014-1069-3

Zarei, A.R., Eslamian, S. (2017). Trend assessment of precipitation and drought index (SPI) using parametric and non-parametric trend analysis methods (case study: Arid regions of southern Iran).

International Journal of Hydrology Science & Technology 7, 12. https://doi.org/10.1504/IJHST.2017.080957

Yu, G. (2015). Inorganic nitrogen wet deposition: Evidence from the North-South Transect of Eastern China. Environmental Pollution, 204, 1-8. https://doi.org/10.1016/j.envpol.2015.03.016

Zhang, X., Huang, X., Zhao, X., Lu, R., Lai, L. (2009). Effects of land use change on vegetation carbon storage in the taihu lake region. Journal of Natural Resources 2 24, 1343-1353 (in Chinese).

Zhu, J., He, N., Wang, Q., Yuan, G., Wen, D., Yu, G., Jia, Y. (2015). The composition, spatial patterns, and influencing factors of atmospheric wet nitrogen deposition in Chinese terrestrial ecosystems. Sci Total Environ. 511, 777-785. https://doi.org/10.1016/j.scitotenv.2014.12.038

Zhu, W., Pan, Y., He, H., Yu, D., Hu, H. (2006). Simulation of maximum light use efficiency for some typical vegetation types in China. Chinese Science Bulletin, 51, 457-463(in Chinese).

Zhu, W., Pan, Y., Zhang, J. (2007). Estimation of net primary productivity of chinese terrestrial vegetation based on remote sensing. Chinese Journal of Plant Ecology 31, 413-424 (in Chinese).